The Enhanced Drying Effect of Central-Pacific El Niño on US Winter

Jin-Yi Yu* and Yuhao Zou

Department of Earth System Science

University of California, Irvine, CA

January, 2013

Revised, *Environmental Research Letters*

---

*. *Corresponding author address*: Dr. Jin-Yi Yu, Department of Earth System Science, University of California, Irvine, CA 92697-3100. E-mail: jyyu@uci.edu

ABSTRACT

In what is arguably one of the most dramatic phenomena possibly associated with climate change or natural climate variability, the location of El Niño has shifted more to the central Pacific in recent decades. In this study, we use statistical analyses, numerical model experiments, and case studies to show that the Central-Pacific El Niño enhances the drying effect, but weakens the wetting effect, typically produced by traditional Eastern-Pacific El Niño events on the US winter precipitation. As a result, the emerging Central-Pacific El Niño produces an overall drying effect on the US winter, particularly over the Ohio-Mississippi Valley, Pacific Northwest, and Southeast. The enhanced drying effect is related to a more southward displacement of tropospheric jet streams that control the movements of winter storms. Results from this study imply that the emergence of the Central-Pacific El Niño in recent decades may be one factor contributing to the recent prevalence of extended droughts in the US.

1. Introduction

The climate in the United States (US) is significantly influenced by El Niño events in the tropical Pacific (e.g., Ropelewski and Halpert 1986; 1989, Kiladis and Diaz 1989; Livezey et al. 1997; Dettinger et al. 1998; Mo and Higgins 1998; Montroy et al. 1998; Cayan et al. 1999; Larkin and Harrison 2005b; and many others). The influences on the winter climate are often described as a seesaw pattern as the northern US tends to be warmer and drier than normal while the southern US tends to be colder and wetter than normal. However, the recent recognition of the existence of two types of El Niño (Wang and Weisberg 2000; Trenberth and Stepaniak 2001; Larkin and Harrison 2005a; Yu and Kao 2007; Ashok et al. 2007; Guan and Nigam 2008; Kao and Yu 2009; Kug et al. 2009) has prompted efforts to refine this classical view and to differentiate the impacts according to the El Niño type. The two different El Niño types that have recently been emphasized are the Eastern-Pacific (EP) El Niño and the Central-Pacific (CP) El Niño (Yu and Kao 2007; Kao and Yu 2009). EP El Niño events are characterized by sea surface temperature (SST) anomalies extending along the equator westward from the South American Coast, while the CP El Niño events are characterized by SST anomalies mostly confined to a region near the equator around the international dateline. While the EP type used to be considered the conventional type of El Niño, the CP type has occurred more frequently in the past few decades (Ashok et al. 2007; Kao and Yu 2009; Kug et al. 2009; Lee and McPhaden 2010; Yu et al. 2012a). The shift in the location of the SST anomalies can lead to different atmospheric responses (Kumar and Hoerling 1995; Mo and Higgins 1998; Hoerling and Kumar 2002; Basugli and Sardeshmukh 2002; DeWeaver and Nigam 2004) to these two types of El Niño and result in different impacts on US climate.

Two recent studies (Mo 2010 and Yu et al. 2012b), for example, have shown that the El Niño impacts on US winter temperatures are different for the CP and EP types and that the typical warm-north, cold-south impact pattern is a mixture of the different impacts produced by the two types of El Niño. According to the studies, different temperature impacts are produced because different wave trains are excited in the extratropical atmosphere when the El Niño SST anomalies are located near the international dateline (CP type) as opposed to near the South American coast (EP type). The CP El Niño excites a wave train resembling the Pacific/North American (PNA; Wallace and Gutzler, 1981) pattern, while the EP El Niño excites a polarward wave train emanating straight out of the tropics into higher latitudes (see Fig. 5 of Yu et al. 2012b). The different wave train responses can also affect the locations and strengths of tropospheric jet streams that control the winter storm paths over the US. In this study, we conduct statistical analyses of reanalysis data, numerical experiments with a forced atmospheric general circulation model, and case studies of the major El Niño events since 1948 to examine the impacts of the two types of El Niño on US winter precipitation.

2. Data and Analysis Methods

This study uses two data products for the analyses: SSTs from the National Oceanic and Atmospheric Administration (NOAA)'s Extended Reconstructed Sea Surface Temperature (ERSST) V3b dataset (Smith and Reynolds 2003) and precipitation and wind data from the National Centers for Environmental Prediction–National Center for Atmospheric Research (NCEP–NCAR) Reanalysis (Kistler et al. 2001). Monthly SST, precipitation, and wind anomalies from 1948 to 2010 were analyzed. Anomalies are defined as deviations from the 1948-2010 climatology.

Monthly values of the EP Niño index and the CP El Niño index from Yu et al. (2012) were used to represent the intensities of the two types of El Niño. The indices were constructed from the monthly SST data using a regression- EOF analysis (Kao and Yu 2009; Yu and Kim 2010). In this method, the SST anomalies regressed with the Niño1+2 (0°-10°S, 80°W-90°W) SST index were removed before the EOF analysis was applied to obtain the spatial pattern of the CP El Niño. The regression with the Niño1+2 index was used as an estimate of the influence of the EP El Niño and was removed to better reveal the SST anomalies associated with the CP El Niño. Similarly, we subtracted the SST anomalies regressed with the Niño4 (5°S-5°N, 160°E-150°W) index (i.e., representing the influence of the CP El Niño) before the EOF analysis was applied to identify the leading structure of the EP El Niño. Figure 1 shows the leading EOF modes obtained from this analysis that exhibit the typical SST anomaly patterns of these two types of El Niño. For the EP El Niño (Figure 1a), the warm anomalies extend from the South American coast to the central Pacific. As for the CP El Niño (Figure 1b), the warm anomalies are confined in the tropical central Pacific near the international dateline. The associated principal components from these two leading EOF modes represent the strengths of these two types of El Niño and are defined as the CP El Niño index and the EP El Niño index, respectively.

We also conducted three ensemble forced experiments with an atmospheric general circulation model (AGCM) to contrast the impacts produced by the two types of

El Niño. The AGCM used is the Version 4 of the Community Atmosphere Model (CAM4) from the National Center for Atmospheric Research. The three experiments include a control run, an EP run, and a CP run. In the control run, climatological, annually-cycled SSTs (calculated from 1948-2010) are used as the boundary condition to force CAM4. For the EP (CP) run, the CAM4 is forced by SSTs constructed by adding together the climatological SSTs and SST anomalies associated with the EP (CP) El Niño. The SST anomalies used in the latter two experiments are constructed by regressing tropical Pacific anomalies with the EP and CP El Niño indices and then scaling them to typical El Niño magnitudes. For each of the runs, a 10-member ensemble of 22-month-long integrations was conducted with the El Niño SST anomalies evolving through a developing phase, peak phase, and decaying phase. The peak phases of the SST anomalies were placed in December of Year 1 for each member.

3. Results

We first regressed US winter (January-February-March; JFM) precipitation anomalies to the EP and CP El Niño indices to identify the impact patterns. The regression coefficients with the US winter precipitation are displayed in Figures 2a-b, with the hatches indicating the data points where the coefficients pass the student-t test at the 90% significance level. The figures show that both types of El Niño produce a dry-north, wet-south anomaly pattern, similar to the seesaw pattern that has traditionally been used to describe the El Niño impacts on US winter precipitation. The dry and wet anomalies are largely along the eastern and western sea boards, with the dry anomalies located mostly over the Pacific Northwest and the Great Lakes regions and the wet anomalies located over the Southwest and the Southeast. However, the intensity and the area coverage of the dry and wet anomalies are noticeably different between the two types. The dry anomalies produced by the CP El Niño are of larger magnitudes and cover larger areas than those produced by the EP El Niño. The areas of dry anomalies expand southward to a greater extent during CP El Niños than during EP El Niños. For example, the dry anomalies cover only the Great Lakes region during EP El Niños, but extend southwestward through the Ohio-Mississippi Valley toward the Gulf Coast during CP El Niños. In contrast, the wet anomalies tend to have smaller magnitudes during CP El Niños than during the EP El Niños—a phenomenon that appears most obviously over the Southeast US. Figures 2a-b indicate that the CP El Niño tends to intensify the dry anomalies but weaken the wet anomalies of the impact pattern produced by the EP El Niño. This important difference is clearly revealed in Figure 2c, where the precipitation anomalies regressed with the EP El Niño were subtracted from the anomalies regressed with the CP El Niño (i.e., Figure 2b minus Figure 2a). Figure 2c shows negative differences over most of the US, excluding the southern portion of the Southwest where positive differences exist. The negative values in Figure 2c indicate that a shift in El Niño from the EP type to the CP type makes the dry anomalies over the Pacific Northwest and along the Ohio-Mississippi Valley drier and the wet anomalies over the Southeast less wet. Southern California and Arizona are the only regions where the CP El Niño makes the winter climate wetter than during the EP El Niño events. Overall, the regression analyses reveal that the CP type of El Niño enhances the drying effect of El Niño on US winter precipitation.

To further confirm the different impacts produced by the two types of El Niño, we examined US winter precipitation anomalies during individual EP and CP El Niño years over the following four regions: the Pacific Northwest, Ohio-Mississippi Valley, Southeast, and Southwest. Yu et al. (2012b) have identified twenty-one major El Niño events during 1948-2010 using the Ocean Niño Index and have determined the types of these events based on the consensus of three different identification methods (Kao and Yu 2009, Yeh et al. 2009, and Ashok et al. 2007). According to their Table 1, eight of the twenty-one El Niño events are of the EP type (1951-52, 1969-70, 1972-73, 1976-77, 1982-83, 1986-87, 1997-98, and 2006-07) while the other thirteen are of the CP type (1953-54, 1957-58, 1958-59, 1963-64, 1965-66, 1968-69, 1977-78, 1987-88, 1991-92, 1994-95, 2002-03, 2004-05, and 2009-10). Figures 2g-i show the US winter precipitation anomalies composited from these two groups of El Niño events. The dry and wet anomalies produced by these El Niño composites are similar, in general, to the regression results shown in Figs. 2a-c that include not only El Niño but also La Niña impacts on US. The composites show dry-north, wet-south patterns for the both types of El Niño, but with the dry anomalies intensified in the CP El Niño composite over the Pacific Northwest and the Ohio-Mississippi Valley and the wet anomalies weakened over the Southeast US.

We then examine in Figure 3 the winter precipitation anomalies in each of these two groups of El Niño events over the four US regions. The specific grid points used in the averages for each of the regions are indicated in the figure. These points were selected from Figure 2 based on the precipitation anomaly centers associated with the both types of El Niño. The stronger drying effect of the CP El Niño over the Pacific Northwest is obvious in Figure 3, which shows a mean precipitation anomaly of -4.3 mm/day for the CP El Niño years but a mean of +1.5 mm/day for the EP El Niño years. Negative anomalies also tend to occur over the Pacific Northwest more consistently during the CP El Niño years (i.e., 10 out of 13 events; 77%) than during the EP El Niño years (i.e., 4 out of 8 events; 50%). This enhanced drying tendency is also very obvious in the Ohio-Mississippi Valley. During eleven of the thirteen CP El Niño years (i.e., 85%), the winter precipitation anomalies over this region are below normal, but the percentage drops to five out of eight (63%) for the EP El Niño years. The mean precipitation anomalies also change from -10.3 mm/day during the CP El Niño group to +0.8 mm/day for the EP El Niño group. Over the Southeast, both types of El Niño produce wet anomalies; however the precipitation anomalies are very large (with a mean value of +12.4 mm/day) during the EP El Niño winters, but are consistently small during the CP El Niño winters (with a mean value of +4.2 mm/day). This is consistent with the conclusion we draw from Figure 2 that the wet anomalies produced by El Niño over the Southeast are weaker during the CP type than during the EP type. Over the Southwest region, positive precipitation anomalies occurred during nine out of the thirteen CP El Niño years (i.e., 69%) and during five out of eight EP El Niño years (62%). The mean precipitation anomalies are +6.6 mm/day for the EP El Niño group and +6.7 mm/day for the CP El Niño group. There are indications of a stronger wetting effect produced by the CP El Niño than the EP El Niño, but the differences are not as significant as those found in the other three regions.

Winter precipitation over the US is primarily associated with winter storms, whose paths across the US are controlled by the locations of tropospheric jet streams. The climatological locations of the jet streams in the winter can be identified by the local maxima in the mean zonal winds at 300mb (U_{300mb}), as shown in Figure 4a. The figure shows that there is a double-jet feature over the west coast that merges into a single-jet over the East Coast (indicated by the black bold lines in the figure). We then separately regressed winter U_{300mb} anomalies onto the EP and CP El Niño indices in Figures 4b and 4c to examine how the jet streams respond to El Niño. The mean locations of the polar and subtropical jet streams identified in Figure 4a are superimposed on Figures 4b-c to aid the examination of the jet stream variations. Figures 4b and 4c indicate that the jet streams shift southward during both types of El Niño, with large negative wind anomalies in the northern US and large positive wind anomalies in the south. Previous studies have suggested that such an equator-ward shift of the tropospheric jet streams during El Niño events result from El Niño-induced Rossby wave trains and strengthening of the Hadley circulation (e.g., Wang and Fu 2000; Seager et al. 2003; Lu et al. 2008). As the jet streams shift southward, winter storms shift south with them, leading to a dry-north, wet-south pattern of precipitation anomalies during the El Niño. However, we find from Figure 4 that the jet streams are displaced more southward during CP El Niños than during EP El Niños. Off the West Coast, for example, the weakening of the zonal winds in the north and the strengthening of the winds in the south are centered, respectively, at 55°N and 30°N for the EP El Niño, but at 45°N and 20°N for the CP El Niño. The more southward displacements of the jet streams explain why the dry anomalies over the northern US (including the Northwest and Ohio-Mississippi Valley) expand and strengthen more significantly during CP El Niños than during EP El Niños. Similarly, the wet anomalies over the southern US expand over the Southwest and extend into the Mexico during the CP El Niño. However, the same southward displacements over the East Coast push the core of the subtropical jet stream (and therefore the storm tracks) out of the US continent and into the Gulf and Caribbean, which results in only a small area of wet anomalies left in the Southeast US during the CP El Niño.

To further verify the different impacts of the two types of El Niño, we contrast in Figures 2d-f the US winter precipitation anomalies calculated from the three forced AGCM ensemble experiments. The impacts produced by the EP and CP types of El Niño on the US winter precipitation were identified by subtracting the ensemble mean of the control run from the ensemble means of the EP and CP runs. It is encouraging to find that the CAM4 experiments reproduce the major findings obtained from the regression analyses (c.f., Figures 2a-c): the CP El Niño enhances the dry impacts and weakens the wet impacts on US winter, except over the Southwest. Compared to the EP run, the CP run produces stronger dry anomalies over the US Northwest and Ohio-Mississippi Valley and weaker wet anomalies over the Southeast. It is particularly interesting to note that the CP run reproduces the strong dry anomalies along the Ohio-Mississippi Valley previously revealed in the analysis of NCEP-NCAR reanalysis (cf. Figures. 2e and 2b). The tendency toward wetter anomalies over the Southwest during the CP El Niño is more evident in the forced CAM4 experiments than in the regression results. We also examined the 300mb zonal wind (U_{300mb}) anomalies from the forced AGCM experiments (shown in Figs. 4e-f) and noted that similar southward shift of the jet streams during the two types of El Niño can be seen in these model results. Particularly, the jet streams in the CP El Niño run displace more southward over the eastern half of the US than in the EP El Niño run, which is consistent with the result obtained from the regression analysis with the reanalysis product. It should be noted that the model zonal wind anomalies are calculated by subtracting the ensemble-mean produced by the control run from the ensemble means produced by the EP and CP run. The U_{300mb} climatology produced by the CAM4 model over the US is reasonably realistic (Fig. 4d).

4. Conclusions

We performed analyses with reanalysis products and numerical experiments to show that the recently-emerged CP type of El Niño can enhance the dry impacts and weaken the wet impacts produced by the traditional EP type of El Niño on US winter precipitations. While both types of El Niño shift the jet streams southward from their climatological winter locations over the US, the shift is larger during the CP El Niño. Since the paths that winter storm moves over the US continent are steered by the jet streams, the more southward shift of the jet streams explains why the dry anomalies that El Niño typically produced over the Pacific Northwest and Ohio-Mississippi Valley expand their covering areas and increase their intensities during the CP El Niño. The more southward shifts of the jet streams are supposed to increase the storm activities and the winter precipitations over the Southwest and Southeast. However, the core of the jet streams along the eastern US moves to the Gulf during the CP El Niño and reduces the land area of wet anomalies over the US Southeast. The Southern end of the Southwest is the only region of the US that is exempted from the drying effect produced by El Niño when it shifts from the EP type to the CP type.

One major implication from this study is that droughts occurred in the Ohio-Mississippi Valley and Pacific Northwest during El Niño years may be intensified after the El Niño becomes more of the CP types, and the Southeast cannot expect as much supply of winter precipitations during El Niño years as in the past. At the same time, the Southwest should prepare for more severe flooding events during CP El Niño years. Another major implication from this study is that the shift of the El Niño from the EP type to the CP El Niño in recent decades may have produced a net drying effect on the US winter precipitations, except over the Southwest. Since the CP El Niño is suggested to occur more frequently in the recent decades, particularly after the 1990, its possible linkage with the extended US drought since the 1990s deserves further investigations.

Acknowledgments. We thank the anonymous reviewers for their valuable comments. This research was supported by NOAA-MAPP Grant NA11OAR4310102 and NSF Grant ATM-1233542.

REFERENCES

Ashok, K., S. K. Behera, S. a. Rao, H. Weng, and T. Yamagata (2007), El Niño Modoki and its possible teleconnection, *Journal of Geophysical Research*, *112*(C11), doi:10.1029/2006JC003798.

Barsugli, J. J., and P. D. Sardeshmukh (2002): Global atmospheric sensitivity to tropical SST anomalies throughout the Indo-Pacific basin. *J. Climate*, **15**, 3427-3442.

Cayan, D. R., K. T. Redmond, and L. G. Riddle (1999), ENSO and Hydrologic Extremes in the Western United States, *Journal of Climate*, **12**, 2881–2893.

Dettinger, M. D., D. R. Cayan, H. F. Diaz, and D. M. Meko (1998), North–South Precipitation Patterns in Western North America on Interannual-to-Decadal Timescales, *Journal of Climate*, **11**, 3095–3111.

DeWeaver, E., S. Nigam (2004), On the Forcing of ENSO Teleconnections by Anomalous Heating and Cooling. *J. Climate*, **17**, 3225–3235.

Guan, B., and S. Nigam (2008), Pacific sea surface temperatures in the twentieth century: an evolution-centric analysis of variability and trend, *Journal of Climate*, **21**, 2790–2809.

Hoerling, M. P. & Kumar, A. (2002), Atmospheric Response Patterns Associated with Tropical Forcing. *Journal of Climate,* **15**, 2184–2203.

Kao, H.-Y., and J.-Y. Yu (2009), Contrasting Eastern-Pacific and Central-Pacific Types of ENSO, *Journal of Climate*, **22**, 615–632.

Kiladis, G. N., and H. F. Diaz (1989), Global Climatic Anomalies Associated with Extremes in the Southern Oscillation, *Journal of Climate*, **2**, 1069–1090.

Kistler, R. et al. (2001), The NCEP–NCAR 50–Year Reanalysis: Monthly Means CD–ROM and Documentation, *Bulletin of the American Meteorological Society*, **82**, 247–267.

Kug, J.-S., F.-F. Jin, and S.-I. An (2009), Two Types of El Niño Events: Cold Tongue El Niño and Warm Pool El Niño, *Journal of Climate*, **22**, 1499–1515.

Kumar, A., and M. P. Hoerling (1995), Prospects and limitations of seasonal atmospheric GCM predictions. *Bull. Amer. Meteor.Soc.*, **76,** 335–345.

Larkin, N. K., and D. E. Harrison (2005a), Global seasonal temperature and precipitation anomalies during El Niño autumn and winter, *Geophysical Research Letters*, **32**, doi:10.1029/2005GL022860.

Larkin, N. K., and D. E. Harrison (2005b), On the definition of El Niño and associated seasonal average U.S. weather anomalies, *Geophysical Research Letters*, **32**, L13705, doi:10.1029/2005GL022738.

Lee, T., and M. J. McPhaden (2010), Increasing intensity of El Niño in the central-equatorial Pacific, *Geophysical Research Letters*, **37**, doi:10.1029/2010GL044007.

Livezey, R. E., M. Masutani, A. Leetmaa, H. Rui, M. Ji, and A. Kumar (1997), Teleconnective response of the Pacific-North American region atmosphere to large central equatorial Pacific SST anomalies, *Journal of Climate*, **10**, 1787–1820.

Lu, J., G. Chen, and D. M. W. Frierson (2008), Response of the Zonal Mean Atmospheric Circulation to El Niño versus Global Warming, *Journal of Climate*, **21**, 5835–5851.

Mo, K. C. (2010), Interdecadal Modulation of the Impact of ENSO on Precipitation and Temperature over the United States, *Journal of Climate*, **23**, 3639–3656.

Mo, K. C., and R. W. Higgins (1998), The Pacific–South American Modes and Tropical Convection during the Southern Hemisphere Winter, *Monthly Weather Review*, **126**, 1581–1596.

Mo, K. C., and R. W. Higgins (1998): Tropical convection and precipitation regimes in the western United States. *J. Climate*, **11**, 2404-2423.

Montroy, D. L., M. B. Richman, and P. J. Lamb (1998), Observed nonlinearities of monthly teleconnections between tropical Pacific sea surface temperature anomalies and central and eastern North American precipitation, *Journal of Climate*, **11**, 1812–1835.

Ropelewski, C. F., and M. S. Halpert (1986), North America precipitaion and temperature associated with the El Niño/Southern Oscillation(ENSO), *Mon Wea Rev*, *114*, 2352–2362.

Ropelewski, C. F., and M. S. Halpert (1989), Precipitation Patterns Associated with the High Index Phase of the Southern Oscillation, *Journal of Climate*, **2**, 268–284.

Seager, R., N. Harnik, Y. Kushnir, W. Robinson, and J. Miller (2003), Mechanisms of Hemispherically Symmetric Climate Variability, *Journal of Climate*, **16**, 2960–2978.

Smith, T. M., and R. W. Reynolds (2003), Extended Reconstruction of Global Sea Surface Temperatures Based on COADS Data (1854 – 1997), *Journal of Climate*, **16**, 1495–1510.

Trenberth, K. E. & Stepaniak, D. P. (2001), Indices of El Niño Evolution. *Journal of Climate*, **14**, 1697–1701.

Wallace, J. M., and D. S. Gutzler (1981), Teleconnections in the Geopotential Height Field during the Northern Hemisphere Winter, *Monthly Weather Review*, **109**, 784–812.

Wang, C. & Weisberg, R. H. (2000), The 1997 – 98 El Niño Evolution Relative to Previous El Niño Events. *Journal of Climate*, **13**, 488–501.

Wang, H. & Rong, F (2000), Influences of ENSO SST Anomalies and Winter Storm Tracks on the Interannual Variability of Upper-Troposphere Water Vapor over the Northern Hemisphere Extratropics. *Journal of Climate*, **13**, 59–73.

Yeh, S.-W., J.-S. Kug, B. Dewitte, M.-H. Kwon, B. P. Kirtman, and F.-F. Jin (2009), El Niño in a changing climate., *Nature*, **461**, 511–514.

Yu, J.-Y., and H.-Y. Kao (2007), Decadal changes of ENSO persistence barrier in SST and ocean heat content indices: 1958–2001, *Journal of Geophysical Research*, **112**, doi:10.1029/2006JD007654.

Yu, J.-Y., and S. T. Kim (2010), Three evolution patterns of Central-Pacific El Niño, *Geophysical Research Letters*, **37**, doi:10.1029/2010GL042810.

Yu, J.-Y., M.-M. Lu, and S. T. Kim (2012a), A change in the relationship between tropical central Pacific SST variability and the extratropical atmosphere around 1990, *Environmental Research Letters*, **7**, 034025, doi:10.1088/1748-9326/7/3/034025.

Yu, J.-Y., Y. Zou, S. T. Kim, and T. Lee (2012b), The changing impact of El Niño on US winter temperatures, *Geophysical Research Letters*, **39**, L15702, doi:10.1029/2012GL052483.

List of Figures

Figure 1. EOF patterns of sea surface temperature anomalies obtained from a regression-EOF method for: (a) the EP type of El Niño and (b) the CP type of El Niño.

Figure 2. US winter (January-February-March; JFM) precipitation anomalies associated with the El Niño are shown in the top panels for the EP El Niño, in the middle panels for the CP El Niño, and in the bottom panels for the difference between the two types of El Niño (i.e., CP impact minus EP impact). The values shown in the left column (a-c) are obtained by regressing US winter precipitation anomalies to the EP and El Niño index. The values shown in the second column (d-f) are calculated by subtracting the ensemble-mean winter precipitation of the forced AGCM experiments from the ensemble means of the EP and CP runs. The values shown in the right column (g-i) are obtained by compositing major EP and CP El Niño events that have occurred since 1950. Values shown are in units of mm/day, and areas passed 90% significance test using a student-t test are hatched.

Figure 3. Winter precipitation anomalies averaged separately for the four selected US regions during the 8 major EP El Niño years and the 13 CP El Niño events. The mean anomalies averaged over the EP or CP El Niño events are also shown in the panels in unit of mm/day.

Figure 4. 300mb zonal winds (U_{300mb}) from NCEP/NCAR reanalysis averaged during the winter season (JFM) from 1948 to 2010 (a), and the anomalies regressed to (b) the EP El Niño index and (c) the CP El Niño index. Panels d-f show, respectively, the ensemble-

mean winter U_{300mb} produced by the control run of the forced AGCM experiment, the U_{300mb} differences between the EP El Niño run and the control run, and the differences between the CP El Niño run and the control run. The climatological locations of tropospheric jet streams are indicated by black bold lines along the local maxima of U_{300mb}. Units shown are in units of m/s.

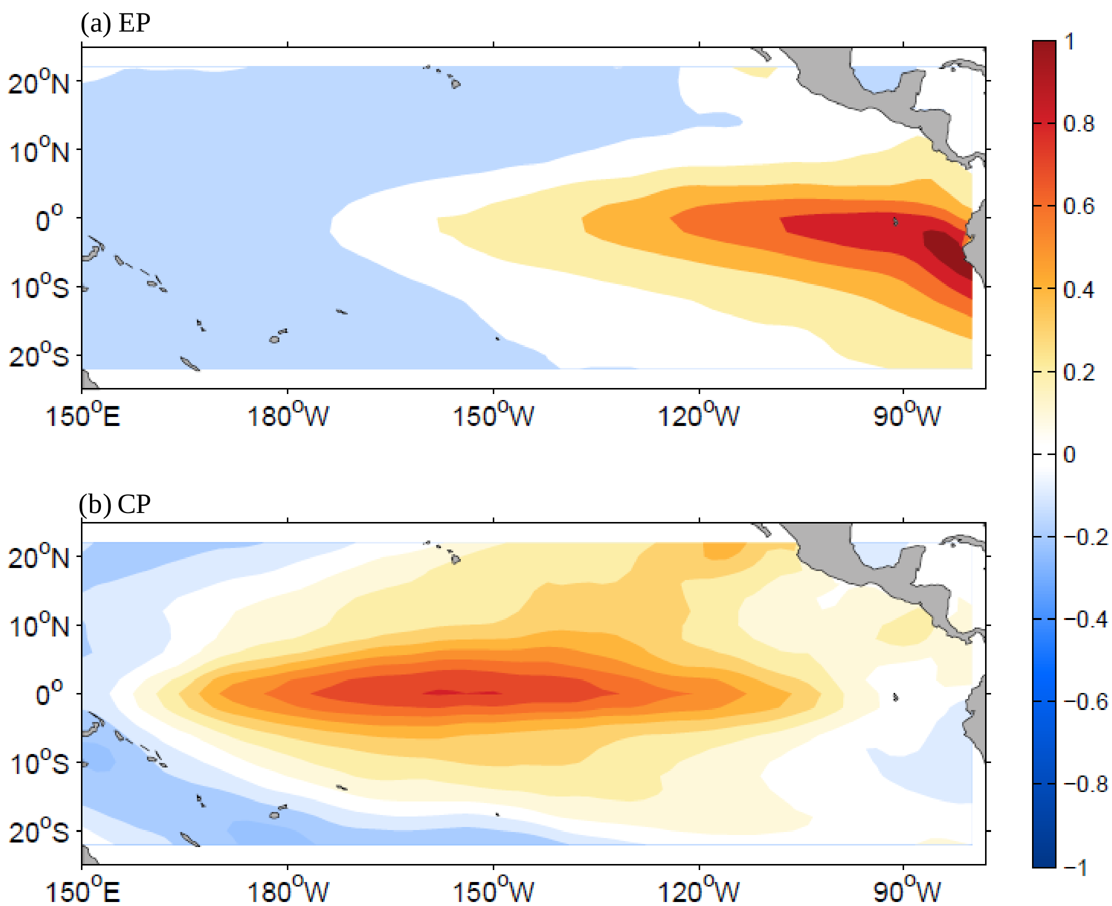

Figure 1. EOF patterns of sea surface temperature anomalies obtained from a regression-EOF method for: (a) the EP type of El Niño and (b) the CP type of El Niño.

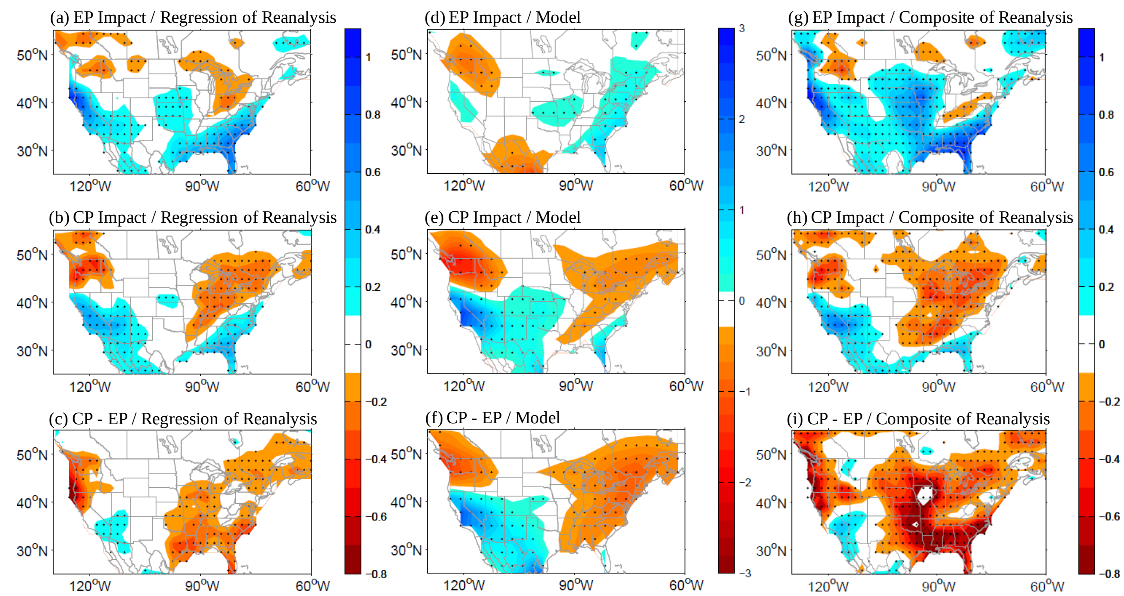

Figure 2. US winter (January-February-March; JFM) precipitation anomalies associated with the El Niño are shown in the top panels for the EP El Niño, in the middle panels for the CP El Niño, and in the bottom panels for the difference between the two types of El Niño (i.e., CP impact minus EP impact). The values shown in the left column (a-c) are obtained by regressing US winter precipitation anomalies to the EP and El Niño index. The values shown in the second column (d-f) are calculated by subtracting the ensemble-mean winter precipitation of the forced AGCM experiments from the ensemble means of the EP and CP runs. The values shown in the right column (g-i) are obtained by compositing major EP and CP El Niño events that have occurred since 1950. Values shown are in units of mm/day, and areas passed 90% significance test using a student-t test are hatched.

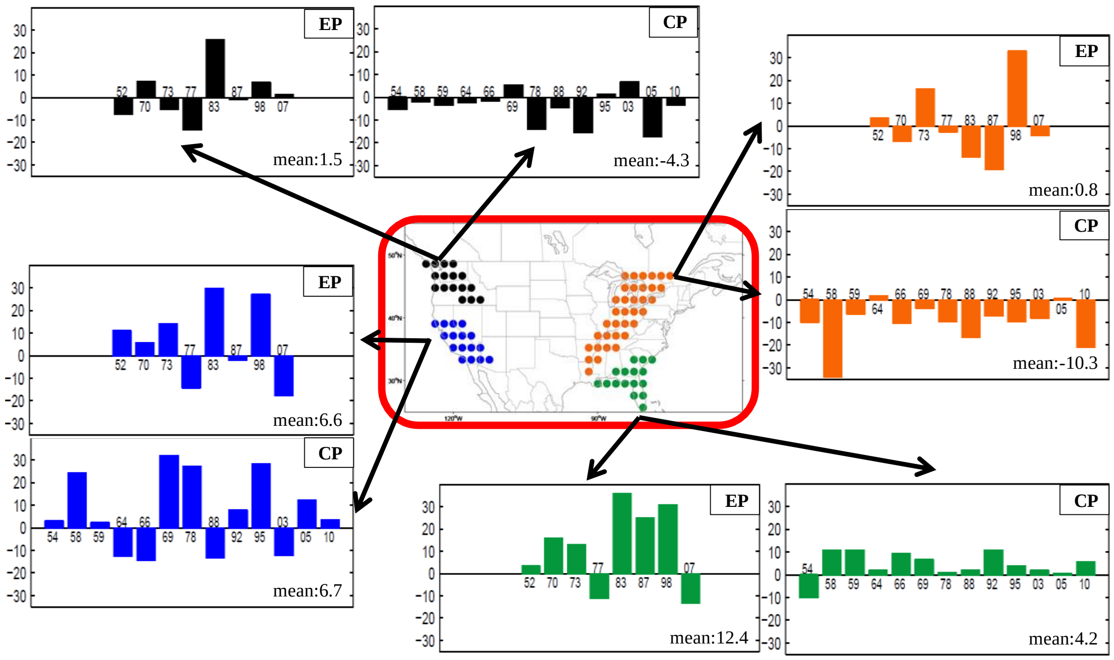

Figure 3. Winter precipitation anomalies averaged separately for the four selected US regions during the 8 major EP El Niño years and the 13 CP El Niño events. The mean anomalies averaged over the EP or CP El Niño events are also shown in the panels in unit of mm/day.

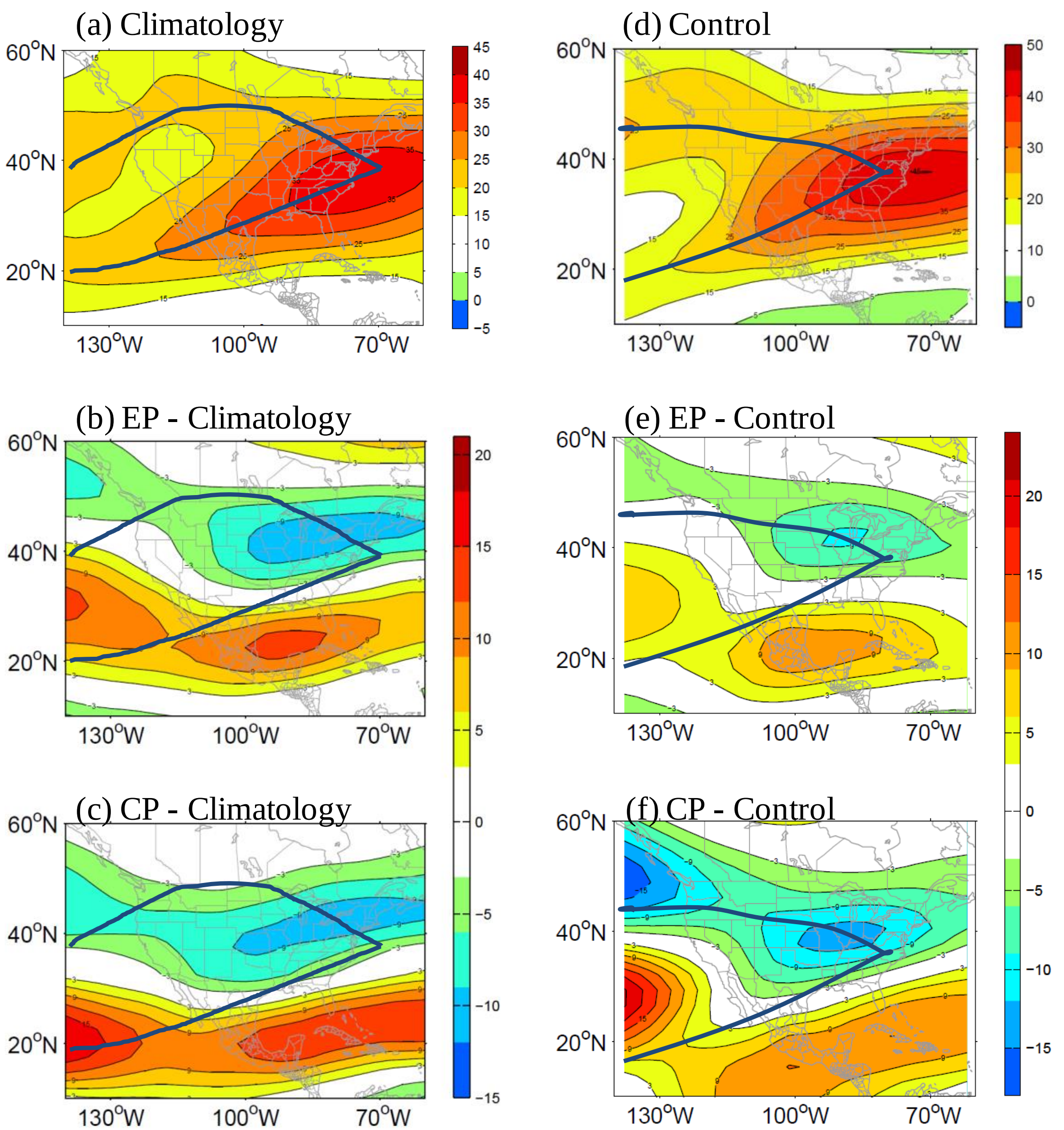

Figure 4. 300mb zonal winds (U_{300mb}) from NCEP/NCAR reanalysis averaged during the winter season (JFM) from 1948 to 2010 (a), and the anomalies regressed to (b) the EP El Niño index and (c) the CP El Niño index. Panels d-f show, respectively, the ensemble-mean winter U_{300mb} produced by the control run of the forced AGCM experiment, the U_{300mb} differences between the EP El Niño run and the control run, and the differences between the CP El Niño run and the control run. The climatological locations of

tropospheric jet streams are indicated by black bold lines along the local maxima of U_{300mb}. Units shown are in units of m/s.